Biodegradation (2007) 18:233–245
DOI 10.1007/s10532-006-9058-6

ORIGINAL PAPER

Contribution to the detection and identification of oxidation metabolites of nonylphenol in *Sphingomonas* sp. strain TTNP3

P. F. X. Corvini · R. Meesters · M. Mundt · A. Schäffer · B. Schmidt · H.-Fr. Schröder · W. Verstraete · R. Vinken · J. Hollender

Received: 12 February 2004 / Accepted: 28 February 2005 / Published online: 5 July 2006
© Springer Science+Business Media B.V. 2006

Abstract *Sphingomonas* sp. strain TTNP3 has been previously described as a bacterium that is capable of degrading the technical mixture of nonylphenol (NP) isomers and also the 4(3′,5′-dimethyl-3′-heptyl)-phenol single isomer of NP. Until recently, 3,5-dimethyl-3-heptanol was the only reported metabolite of 4(3′,5′-dimethyl-3′-heptyl)-phenol. A short time ago, the detection of an intracellular metabolite resulting from the oxidation of 4(3′,5′-dimethyl-3′-heptyl)-phenol which was identified as 2(3,5-dimethyl-3-heptyl)-benzenediol has been reported. A decisive element for this identification was the occurrence of some slight differences with the two most probable metabolites i.e. 4(3′,5′-dimethyl-3′-heptyl)-resorcinol and 4(3′,5′-dimethyl-3′-heptyl)-catechol. These facts led us to hypothesise some NIH shift mechanisms explaining the formation of 2(3′,5′-dimethyl-3′-heptyl)-benzenediol. In the present work, we describe the steps that led to the detection of these metabolites in the intracellular fraction of *Sphingomonas* sp. strain TTNP3. The formation of analogous intracellular metabolites resulting from the degradation of the technical mixture of NP is reported. To further elucidate these degradation products, studies were carried out with cells grown with 4(3′,5′-dimethyl-3′-heptyl)-phenol as sole carbon source. The description of the syntheses of reference compounds, i.e. 4(3′,5′-dimethyl-3′-heptyl)-resorcinol and 4(3′,5′-dimethyl-3′-heptyl)-catechol and their comparative analyses with the intermediates of the degradation of 4(3′,5′-dimethyl-3′-heptyl)-phenol are presented.

Keywords 4(3′,5′-Dimethyl-3′-heptyl)-phenol · Branched isomer · Metabolites · Nonylphenol · Oxidation · *Sphingomonas*

Abbreviations

CID	collision-induced dissociation
NP	nonylphenol
*p*353NC	4(3′,5′-dimethyl-3′-heptyl)-catechol

P. F. X. Corvini (✉) · A. Schäffer · B. Schmidt · R. Vinken
Institute of Environmental Research (Biology V), RWTH Aachen University, Worringerweg 1, D-52056 Aachen, Germany
e-mail: Philippe.Corvini@bio5.rwth-aachen.de

R. Meesters · H.-Fr. Schröder
Department of Environmental Engineering (ISA), RWTH Aachen University, Mies-van-der-Rohe-Strasse 1, D-52074 Aachen, Germany

W. Verstraete
Laboratory of Microbial Ecology and Technology (LabMET), Coupure Links 653, 9000 Ghent, Belgium

M. Mundt · J. Hollender
Institute of Hygiene and Environmental Health, University Hospital-RWTH Aachen, Pauwelsstraße 30, D-52074 Aachen, Germany

*p*353NP	4(3′,5′-dimethyl-3′-heptyl)-phenol (nonylphenol)
*p*353NR	4(3′,5′-dimethyl-3′-heptyl)-resorcinol
tNP	technical nonylphenol

Introduction

As a consequence of the worldwide use of nonylphenol polyethoxylates as additives for a number of industrial product applications, its degradation product, nonylphenol (NP), is an ubiquitous pollutant. Due to its xenoestrogenic potential NP is of primary concern to organisms in the environment and its presence has been widely investigated in technical installations like wastewater treatment plants and their effluents (Giger et al. 1987; Soto et al. 1991; Tanghe et al. 1998). NP has also been detected in aqueous environments such as sea and surface waters and even in the atmosphere above the latter. Furthermore, this xenobiotic compound has also been detected in food and in soils, which were fertilised with sewage sludge or not (Dachs et al. 1999; Ekelund et al. 1993; Espadaler et al. 1997; Liber et al. 1999; Sundaram and Szeto 1981).

NP dissipation or degradation in soil, sediments and aqueous environments has often been reported and attributed essentially to bacteria and sometimes to fungi (Corti et al. 1995; Ekelund et al. 1993; Fujii et al. 2000; Hesselsøe et al. 2001; Tanghe et al. 1999; Topp and Starratt 2000; Vallini et al. 1997). Among them two strains of NP-degrading *Sphingomonas* have been isolated from wastewater treatment plants (Fujii et al. 2001; Tanghe et al. 1999). More recently, *Sphingobium amiense* has been isolated from river sediment which also is capable to degrade NP (Ushiba et al. 2003). Metabolic pathways of NP in these bacterial strains and more generally in other studies remain poorly documented (Fujii et al. 2000; Tanghe et al. 1999; Van Ginkel 1996). The main reason is that NPs industrial production process leads to a wide range of alkyl-chain isomers (more than 20) rendering metabolism studies more difficult (Tanghe et al. 2000; Wheeler et al. 1997). Although no other degradation products than the supposed nonanol have been detected and no aromatic degradation intermediate could be found, some authors hypothesised that NP metabolism by *Sphingomonas* occurs via a ring hydroxylation (Fujii et al. 2000; Tanghe et al. 2000).

In previous studies, we reported the degradation of a chemically synthesised single isomer of NP i.e. the 4(3′,5′-dimethyl-3′-heptyl)-phenol (*p*353NP) in its non-radioactive and uniformly ring-^{14}C-labelled form by *Sphingomonas* sp. strain TTNP3 (Corvini et al. 2004a). It could be demonstrated that the aromatic ring of NP was effectively mineralised to radioactive CO_2. Furthermore, radioactivity was detected in the cells indicating that NP is used by *Sphingomonas* sp. strain TTNP3 for biomass production. In the extracellular medium only 3,5-dimethyl-3-heptanol (nonanol) was identified. This metabolite corresponds with the nonyl chain of *p*353NP, where the aromatic ring has been replaced by a hydroxy function. The mechanism that leads to the formation of nonanol remains to be elucidated. This would imply oxidation of a tetravalent carbon in position 3′ of the nonyl chain (Fig. 1a), which is a considerably stable partial structure of the molecule.

Since the experiments described before (Corvini et al. 2004a) did not allow the detection of any intermediary metabolite other than nonanol in extracts of *Sphingomonas* sp. strain TTNP3 cells and extracellular medium, investigation of the intracellular formation of metabolites by *Sphingomonas* sp. strain TTNP3 was performed. In an overview study concerning the metabolism of this isomer of NP, the detection of intracellular metabolites resulting from the oxidation of NP was briefly reported (Corvini et al. 2004b). Recently, these metabolites have been definitively identified as the 2(3′,5′-dimethyl-3′-heptyl)-benzenediol resulting from a hydroxylation-induced migration of the alkyl chain (NIH shift) (Corvini et al. 2004c). A decisive element for the identification of such unexpected metabolite was the occurrence of some slight differences with the two most probable metabolites i.e. 4(3′,5′-dimethyl-3′-heptyl)-resorcinol (*p*353NR) and 4(3′,5′-dimethyl-3′-heptyl)-catechol (*p*353NC). In the

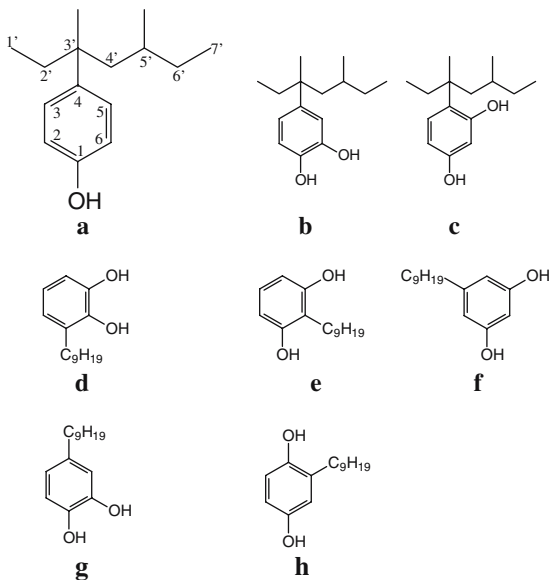

Fig. 1 Reference compounds (**a–c**) and possible metabolites of *p*353NP (**d–h**). (**a**) 4(3′,5′-dimethyl-3′-heptyl)-phenol (*p*353NP); (**b**) 4(3′,5′-dimethyl-3′-heptyl)-catechol (*p*353NC); (**c**) 4(3′,5′-dimethyl-3′-heptyl)-resorcinol (*p*353NR); (**d**) and (**e**) adjacent trisubstituted metabolites; (**f**) symmetrically trisubstituted metabolite; (**g**) nonylcatechol with modified alkyl chain; (**h**) metabolite resulting from a NIH shift

present work, we describe in detail the steps that led to the detection of these metabolites in the intracellular fraction of *Sphingomonas* grown either on technical nonylphenol (tNP) or on *p*353NP in a second time. The detailed chemical synthesis of *p*353NR and *p*353NC and their structural confirmation by NMR spectroscopy are reported. Lastly, the comparative analyses of these intermediates of degradation with the synthesized *p*353NR and *p*353NC are presented.

Materials and methods

Bacterial strain and culture conditions

Sphingomonas sp. strain TTNP3 precultures in complex medium and NP-degrading cultures in mineral medium were prepared as previously described (Corvini et al. 2004a). tNP or the chemically synthesised single NP isomer 4(3′,5′-dimethyl-3′-heptyl)-phenol (*p*353NP) were added as sole carbon source at a concentration of 1 g/l.

For the biodegradability tests of the metabolites, cultures with *p*353NC, and *p*353NR, were prepared under the same conditions. Added amounts of metabolites corresponded to 1 ml extract prepared as described in the next section. The solvent was evaporated before adding 10 ml of mineral medium. For the tests with *p*353NC and *p*353NR, their concentration was adjusted to that of the metabolites. As control experiment *p*353NP was added to a concentration of 100 mg/l.

Isolation of intracellular metabolites

For intracellular studies, crude cell extracts were prepared as follows. In order to work with higher cell-densities, 1.4 l of *Sphingomonas* sp. strain TTNP3 suspension cultivated on tNP was harvested after 15 days of incubation. The cultures with the single isomer were incubated for 6 days. *Sphingomonas* sp. strain TTNP3 cell cultures were centrifuged at 30,000*g* and 4°C for 15 min. Supernatant was discarded and cells were washed two times with 50 ml of phosphate buffer (pH 7.0, 50 mM). After the last centrifugation step, pellets were resuspended in 25 ml of the same phosphate buffer. The cell suspensions containing 16.8 g dry-weight biomass/l were sonicated with an energy supply of 40 W (Branson sonifier II model 250). They were maintained at 4°C during 5 sonication cycles of 75 s (15 s pause between each cycle). Five ml of 1 M HCl were added to the cell lysates. The acidified solution was extracted two times with 50 ml and 25 ml ethyl acetate, respectively, by shaking the mixture vigorously. The combined organic phases were dried over Na_2SO_4 and filtered before being evaporated under a N_2 stream to a final volume of 5 ml. Aliquots of the intracellular extracts were stored at –20°C for further analysis. Prior to GC analysis, 50 µl of the samples were dried under a gentle nitrogen stream, derivatised with 50 µl *N*-methyl-*N*-trimethylsilyltrifluoroacetamide (MSTFA; Fluka) and diluted adequately.

GC-MS analysis and GC-MS-MS analysis

The GC-MS analyses were performed according to Vinken et al. (2002).

The GC-MS-MS analyses were performed with a Finnigan MAT GCQ gas chromatograph (Finnigan MAT, San Jose, USA) equipped with an ion trap mass spectrometric detector operating in the positive electron impact mode (EI+). For analysis 2 µl split injections (1:10) were carried out by auto-sampling (A 200 S auto sampler; Finnigan MAT). The GC separation was performed on a fused silica capillary column (DB-17 ms, film thickness 0.25 µm, 60 m × 0.25 mm I.D; J&W Scientific, Folsom, USA). Helium was used as carrier gas at a linear velocity of 40 cm/s. The injector temperature and the transfer line temperature were set at 250°C and 275°C, respectively. The initial oven temperature was set to 80°C and held for 3 min. Then oven was heated to 280°C by a temperature ramp of 10°C/min and held for 7 min under these conditions. After 35 min of data acquisition, a post analysis baking at 280°C for 3 min was applied to the column. The positive electron impact full scan data were acquired at an ion source temperature of 150°C. Data acquisition was performed for ions at *m/z* 30–450 and a scan time of 1.76 s was applied. The data were acquired after a solvent delay of 8 min. For ionisation, the electron energy was 70 eV. An emission current of 250 μA and an electron multiplier voltage 1,750 V were applied.

For MS/MS analysis the precursor ions at *m/z* 380 were isolated during 14 ms. An excitation voltage of 1.00 V (excitation energy 0.450) was applied during 15 ms and product ions were scanned within a range of *m/z* 190–400.

Gas chromatography/Fourier-transform infrared spectrometry (GC/FTIR)

A Perkin Elmer 8420 gas chromatograph (Rodgau-Jügesheim, Germany) equipped with a Perkin Elmer 1700x GC/FTIR Interface and a Perkin Elmer 1740 Infrared Fourier-Transform spectrometer was used for infrared analysis. Helium was used as carrier gas and a linear gas pressure of 110 kPa was applied. The injector temperature and the transfer line temperature were set to 250°C and 200°C, respectively. For analysis 2 µl split injections (1:10) were carried out manually on a 30 m Quadrex 007 608 column with an I.D. of 0.53 mm and a film thickness of 0.8 µm (New Haven, Connecticut, USA). The initial oven temperature was set to 40°C and held for 4 min before being heated to 280°C by a temperature ramp of 10°C/min and hold for 25 min. The infrared spectra were recorded at a scan speed of 2.0 cm/s and at a resolution of 8 cm^{-1}. The scan ranged from 4,000 to 700 cm^{-1}.

HPLC-DAD-MS

The samples were analysed by HPLC with UV diode-array (HP 1100, Hewlett Packard) and electrospray ionisation mass spectrometry detectors in series (ESI-MS, SSQ 7000, Finnigan MAT). A reversed-phase Nucleosil 100 C18-column was used (particle size 5 µm, 4.1 × 250 mm^2; Alltech) with methanol and H_2O as the mobile phase at a flow rate of 0.6 ml/min. A gradient from 70% to 80% (v/v) methanol within 15 min, hold for 5 min, from 80% to 100% within 5 min, hold for 4 min and from 100% to 70% within 6 min was employed. UV-detection was performed at 210 nm with spectra acquisition from 190 nm up to 400 nm. A voltage of –4.5 V was applied to the electrospray needle, the capillary temperature was set to 200°C, sheath gas was adjusted to 60 psi and auxiliary gas to 30 psi. Detection was performed in the negative mode using a collision-induced dissociation (CID) of 20 V.

Chemical synthesis of the reference compounds *p*353NC and *p*353NR

The *p*353NR was synthesised by Friedel–Crafts alkylation from resorcinol (Merck, Darmstadt, Germany) and 3,5-dimethyl-3-heptanol (Avocado, Heysham, U.K.). In the case of *p*353NC, guaiacol (Merck, Darmstadt, Germany) and the 3,5-dimethyl-3-heptanol were allowed to react correspondingly in a first step to form nonylguaiacol, followed by demethylation. In all cases, the products consisted of two diastereomers. For the alkylation step, 880 mg of resorcinol, or 440 mg of guaiacol, 700 µl of 3,5-dimethyl-3-heptanol, 5 ml of BF_3–ether complex (Merck,) and 5 ml of diethyl ether for *p*353NR synthesis or 35 ml petroleum ether (boiling range from 60°C to 95°C) in case of guaiacol were

placed in a 100 ml two-necked flask equipped with a reflux condenser and a drying tube filled with $CaCl_2$. Petroleum ether and diethyl ether (Acros, New Jersey, USA) were dried over molecular sieve 4 Å prior to use. The reaction was allowed to run for 90 min (*p*353NR synthesis), or 30 min (nonylguaiacol synthesis) at 40°C with stirring. Then the reaction was stopped by addition of one volume of distilled water and the mixture was stirred intensely for further 15 min. The aqueous phase was removed and the organic phase was washed 5 times with one volume of 0.1 M HCl in order to remove the non-reacted educts, and then dried over Na_2SO_4 (Acros). After removing the solvent under vacuum, the product yields were 356 mg of pure nonylguaiacol and for *p*353NR 635 mg with a purity of 90.1%. The latter included dialkylated resorcinol as by-product (GC-MS analysis). The nonylguaiacol product was further demethylated with 3 ml of 1 M BBr_3 solution in CH_2Cl_2 (Fluka) in 30 ml of petroleum ether at 50°C for 90 min in the same apparatus. After stopping the reaction with one volume of distilled water, the mixture was treated as described above. For identification and characterisation of the reaction products, GC-MS was used. Demethylation was quantitative and led to two diastereomers of pure *p*353NC (GC-MS). For further identification ^{13}C- and ^{1}H-solution state NMR spectra were recorded in $CDCl_3$ on a Varian Inova-400 spectrometer (Varian Inc., Palo Alto, USA) at 100 and 400 MHz, respectively; as internal standard tetramethylsilane (TMS) was used, coupling constants *J* are given in Hz.

Results and discussion

Metabolites of tNP

The aim of this work was to assess the presence of metabolites of NP in the intracellular fraction of *Sphingomonas* sp. strain TTNP3. Because of the low biomass yields of *Sphingomonas* sp. strain TTNP3 grown on tNP as well as on *p*353NP (approx. 300 mg dry weight/l), suspensions with high biomass concentration of *Sphingomonas* sp. strain TTNP3 grown on NP (16.8 g cell dry weight/l) were applied for the preparation of intracellular extracts. Due to the high amount of NP (1.4 g) required for such experiments, these assays were carried out first with bacteria cultivated with tNP. Organic fractions of these intracellular extracts were silylated with MSTFA prior analyses by GC-MS. The chromatogram showed the emergence of a group of many unresolved peaks between 20.7 and 22.4 min (Fig. 2, top), which exhibited a pattern similar to that of tNP, where peaks appeared between 17.9 and 20.3 min (Fig. 2, bottom). The mass spectra analysis of these new peaks demonstrated molecule ions at *m/z* 380 for all compounds of this group, whereas those of derivatised tNP had molecular ions at *m/z* 292. As their corresponding non-derivatised forms, the trimethylsilylated-tNP isomers showed mainly fragmentations at the nonyl-chain by cleavage of alkyl residues (data not shown). The GC-MS fragmentation patterns of the compounds detected in the intracellular extract resembled those of the parent NP isomers. Losses of fragments with masses of 15, 29, 71 and 99 which corresponded to alkyl group fragmentations were detected in their mass spectra. The molecular ion at *m/z* 380 was explained by hydroxylation of the tNP isomers, which led to doubly trimethylsilylated derivatisation products.

The metabolites were also analysed by negative ion LC-MS without derivatization, where usually $(M\text{-}H)^-$ signals are detected. Besides remaining tNP isomers (at *m/z* 219), which gave one large peak, a new broad peak with a pseudo molecule ion at *m/z* 235 and with a maximum of UV absorption at ca. 280 nm was detected in the sample (data not shown). This peak had a shorter retention time (14.5–16.5 min) than tNP (18.5–22.5 min). Under the applied reversed phase chromatography, this indicated that the corresponding metabolites were more hydrophilic than tNP.

Detection of the metabolites of *p*353NP

Because of the difficulty to separate each peak of the tNP-derived metabolites, interpretation of the mass spectra was too complex in the case of tNP. Therefore, further experiments were performed with cultures of *Sphingomonas* sp. strain TTNP3 grown on *p*353NP (Fig. 1a). It is important to

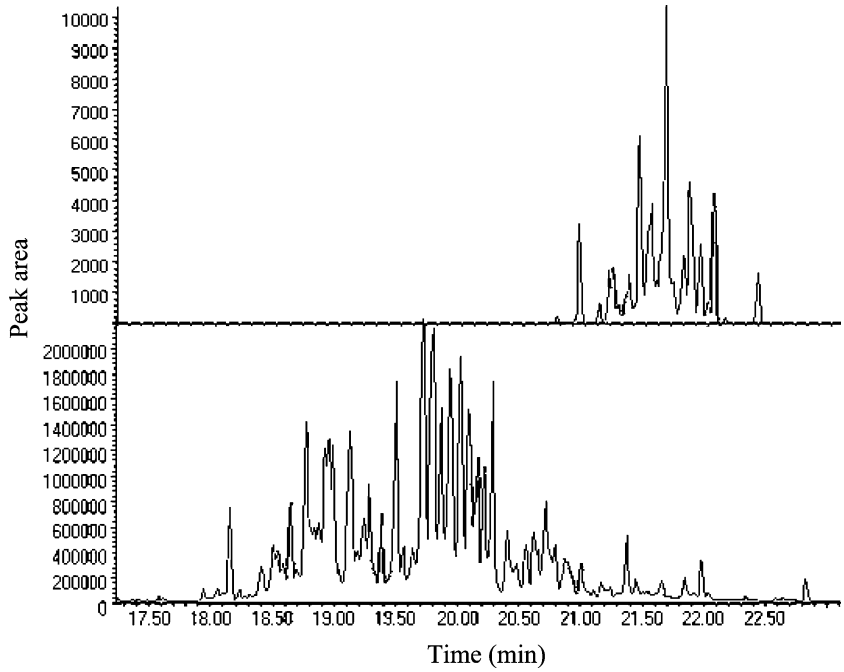

Fig. 2 GC-chromatograms of intracellular extract of *Sphingomonas* sp. strain TTNP3 grown on tNP; total ion (*bottom*) and ion at *m/z* 380 (*top*)

note that due to two asymmetric carbon atoms (C3′ and C5′), *p*353NP consisted of two diastereomers. The latter gave rise to two peaks with the same fragmentation patterns (GC-MS). The use of *p*353NP in the metabolism studies should allow for a simpler chromatographic pattern of the resulting metabolites. Furthermore, metabolites should probably also be present in higher amounts than in cultures grown on tNP.

GC-MS analysis of the extract confirmed the presence of two peaks with molecular ions at *m/z* 380 and retention times of 21.46 and 21.55 min, respectively. Both metabolites displayed the same mass spectrum indicating their origin from the diastereomers of *p*353NP. It was assumed that they were also diastereomers. As previously reported the main ion was found at *m/z* 73 and corresponds to a trimethylsilyl fragment (Corvini et al. 2004c). Prominent ions were observed at *m/z* 267, 281, and 309, which corresponded to alkyl losses. Similar fragmentations (ions at *m/z* 179, 193 and 221) resulted from derivatised *p*353NP (Table 1). As for the parent compound, the main eliminated neutral fragments were M+ –71, M+ –99 and M+ –113. The elimination of these fragments occurred with both, *p*353NP and its metabolites. As already reported (Corvini et al. 2004c), the occurrence of the M+ –113 ion was explained by the formation of substituted tropylium ions and M+ –71 corresponded to the loss of a pentyl fragment. The formation of the substituted tropylium ion is important to notice because it indicates that the hydroxy group is probably attached to the ring. Regarding the M+ –99 ion, fragmentation implies the loss of both an ethyl and a pentyl fragment with a shift of a hydrogen atom to the positive ions. Furthermore, a trace at M+ –126 (*m/z* 254) confirmed that the whole alkyl chain was lost. These facts showed clearly that the additional (derivatised) hydroxy group was attached to the ring.

As observed for the intracellular extract obtained from the cells grown on tNP, negative ion LC-MS analysis of the sample derived from *p*353NP confirmed the presence of a narrow peak with a retention time of 14.9 min and a pseudo molecule ion $(M\text{-}H)^-$ at *m/z* 235 (Corvini et al. 2004b). Moreover, the UV absorption maximum of this peak (around 280 nm) and its entire UV spectrum (Fig. 3) were characteristic for an aromatic ring, and were comparable to those obtained from experiments with tNP.

The experiments thus showed that the metabolites were aromatic ring-oxidation products of

Table 1 Chromatographic and mass spectral characteristics of the trimethylsilylated derivates of: metabolites of *p*353NP, *p*353NC, *p*353NR and *p*353NP

Diastereomers compounds	*m/z*	Relative abundance	M+ –*x*
Metabolites (*p*353NP culture)	73	100	307
trimethylsilylated[a]; Molecule ion = 380;	254	8	126
Retention time 21.45 and 21.55 min	267	23	113
	281	74	99
	309	38	71
	380	27	0
*p*353NC trimethylsilylated;	73	100	307
Molecule ion = 380; Retention	267	3	113
time 21.43 and 21.53 min	281	31	99
	309	59	71
	351	8	29
	380	6	0
*p*353NR trimethylsilylated; Molecule ion = 380;	73	37	307
Retention time 21.62 and 21.73 min	267	9	113
	281	50	99
	309	100	71
	351	13	29
	380	5	0
*p*353NP trimethylsilylated; Molecule ion = 292;	73	60	307
Retention time 19.59 and 19.67 min	179	20	113
	193	67	99
	221	100	71
	263	15	29
	292	4	0

[a]Values taken from Corvini et al. 2004c

*p*353NP. Furthermore, double trimethylsilylation of the metabolites using MSTFA indicates that the parent compound (*p*353NP) was hydroxylated.

Characterisation of the synthesised *p*353NC and *p*353NR

In order to further identify these metabolites, the two most probable hydroxylation products of *p*353NP, i.e. the catechol derivative *p*353NC (Fig. 1b) and the *p*353NR (Fig. 1c) were separately synthesised. Due to the presence of two asymmetric carbons on their respective alkyl chain, both *p*353NC and *p*353NR exist as to two diastereomers, as it is the case for the *p*353NP.

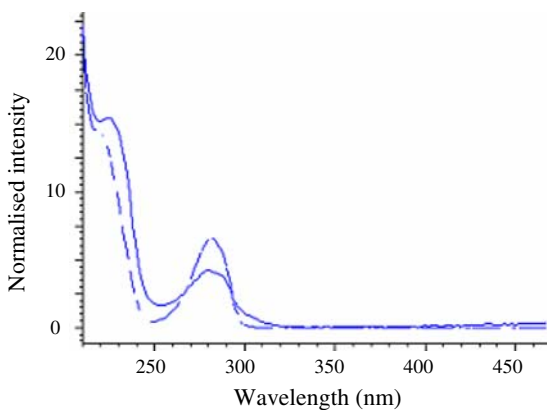

Fig. 3 UV spectra of *p*353NC (*full line*) and metabolites (*dashed line*) acquired during HPLC analysis

For the synthesis of *p*353NC, a direct alkylation of catechol was not possible because alkylation at *meta* position relatively to a hydroxyl group is unfavourable. That is why guaiacol (2-methoxy-phenol) was firstly alkylated at position C4 by using 3,5-dimethyl-3-heptanol in presence of BF_3–ether complex as catalyst. Finally, *p*353NC (purity >99%) was obtained by demethylation of the alkylation product of guaiacol in presence of BBr_3. For the synthesis of *p*353NR, resorcinol was directly alkylated by means of 3,5-dimethyl-3-heptanol in presence of BF_3–ether complex. The purity was above 90% and the main by-product was the dialkylated resorcinol. After verification of the presence of typical diastereomer peaks for both the *p*353NC and the *p*353NR giving M+ ions at *m/z* 380 (double trimethylsilylated) by GC-MS analysis in each reaction mix,

the reference compounds were analysed by ^{13}C- and ^{1}H-solution state NMR.

The ^{1}H-NMR chemical shifts in ppm relative to the internal standard TMS recorded for the two synthesised standard compounds and the resulting coupling constants J (expressed in Hz) were (for positions of atoms see Fig. 1a):

*p*353NC (*diastereomer*): 0.50, 0.75 (each doublet, J = 6.6, 3 H–(CH_3 at C5′)); 0.66, 0.77 (each triplet, J = 7.4, 3 H–C7′); 0.62 (triplet, J = 7.7, 3 H–C1′); 0.87–0.94, 1.00–1.11, 1.16–1.31, 1.39–1.50, 1.59–1.69 (each broad multiplet, 10 H–C(2′, 4′–6′, CH_3 at C3′)); 6.12 (singlet, 2 H–OH); 6.69 (double doublet, J_1 = 8.2, J_2 = 1.9, H–C5); 6.79 (doublet, J = 8.2, H–C6); 6.86 (d, J = 1.9, H–C3).

*p*353NR (*diastereomer*): 0.51, 0.77 (each doublet, J = 6.6, 3 H–(CH_3 at C5′)); 0.59–0.69 (broad multiplet, 6 H–C(1′, 7′)); 0.88–1.00, 1.03–1.15, 1.25–1.32, 1.38–1.49, 1.92–1.98, 2.04–2.21 (each broad multiplet, 10 H–C(2′, 4′–6′, CH_3 at C3′)); 5.06 (doublet, J = 3.9, OH at C3); 5.46 (singlet, OH at C1); 6.21, 6.22 (each d, J = 2.5, H–C2); 6.34 (double doublet, J_1 = 8.5, J_2 = 2.5, H–C6); 6.96, 6.99 (each doublet, J = 8.5, H–C5).

The ^{13}C-NMR chemical shifts in ppm relative to the internal standard TMS of *p*353NC and *p*353NR were (for positions of atoms see Fig. 1a):

*p*353NC (*diastereomer*): 8.790, 8.850 (C1′); 11.437, 11.634 (C7′); 21.481, 21.906 (CH_3 at C5′); 23.051, 23.749 (CH_3 at C3′); 30.743, 30.971 (C5′); 31.540, 32.025 (C6′); 36.183, 36.714 (C2′); 40.969, 41.159 (C3′); 50.763, 50.816 (C4′); 114.637, 114.659 (C3); 115.228 (C6); 119.666, 119.712 (C5); 140.558 (C1); 141.908, 141.946 (C4); 142.834 (C2).

*p*353NR (*diastereomer*): 9.116, 9.154 (C1′); 11.354, 11.589 (C7′); 20.942, 21.860 (CH_3 at C5′); 24.902, 25.274 (CH_3 at C3′); 31.252, 31.312 (C5′); 31.912, 32.041 (C6′); 33.687, 33.823 (C2′); 41.311, 41.515 (C3′); 47.076, 47.182 (C4′); 103.849, 103.887 (C2); 107.043, 107.089 (C6); 125.606, 125.636 (C4); 130.264, 130.302 (C5); 154.091, 154.061 (C3); 155.130, 155.214 (C1).

On the whole, the chemical structures of the synthesised *p*353NC and *p*353NR could be confirmed by their ^{1}H-, ^{13}C-NMR, and mass spectra, which were interpreted comparatively to the ^{1}H- and ^{13}C-NMR analyses of *p*353NP (Vinken et al. 2002).

Mass spectrometric comparison of the metabolites with *p*353NC and *p*353NR

GC-MS analyses were performed for trimethylsilylated *p*353NC and *p*353NR and both reference compounds showed two peaks (Table 1). Retention times of *p*353NC and *p*353NR diastereomers were quite similar to those of the metabolites observed during the experiments with *p*353NP (< 0.1 min difference). *p*353NC appeared shortly before, *p*353NR slightly later than the metabolites. Spiking experiments with the synthesised compounds and the metabolites showed that they differed regarding their retention times. Although the ring substitution patterns of *p*353NC and *p*353NR differed, no evident differences of MS fragments were found. Only differences in the relative abundance of the ions were detected. For *p*353NC the main ion was at *m/z* 73 as for the *p*353NP metabolites, whereas for *p*353NR the main fragment was at *m/z* 309 as for the *p*353NP. As for *p*353NP and its metabolites, fragmentation occurred essentially at the alkyl-chain in the case of *p*353NC and *p*353NR. This resulted in the emergence of the prominent ions at *m/z* 267, 281, 309, 351, and 380.

For further examination, GC-MS-MS analyses were performed by trapping the 380 *m/z* ion for a second ionisation (Fig. 4). Concerning the isolated *p*353NP metabolites the fragments were at *m/z* (relative abundance in %): 380 (24), 351 (5), 323 (10), 322 (22), 309 (100), 281 (90), and 267 (24) (Fig. 4a). For *p*353NC fragmentation pattern was *m/z*: 380 (6), 351 (100), 309 (96), 281 (22) (Fig. 4b) and for *p*353NR *m/z*: 351 (81), 309 (100), and 281 (18) (Fig. 4c). GC-MS-MS thus showed only slight differences between *p*353NC and *p*353NR; the fragmentation of the alkyl chain was not strongly influenced by these substitution patterns of the aromatic ring. Metabolites differed mainly from reference compounds having a very weak *m/z* 351 fragment (ethyl loss), a quite high *m/z* 281 and significant *m/z* 322, 323, and 267 fragments. Fragments *m/z* 322 and 323 may be interpreted as ionisation products resulting from a fragmentation between C4′ and C5′ with or without a H atom shift. The differences observed between GC-MS and GC-MS-MS analysis were explained by the use of two different mass spectrographs.

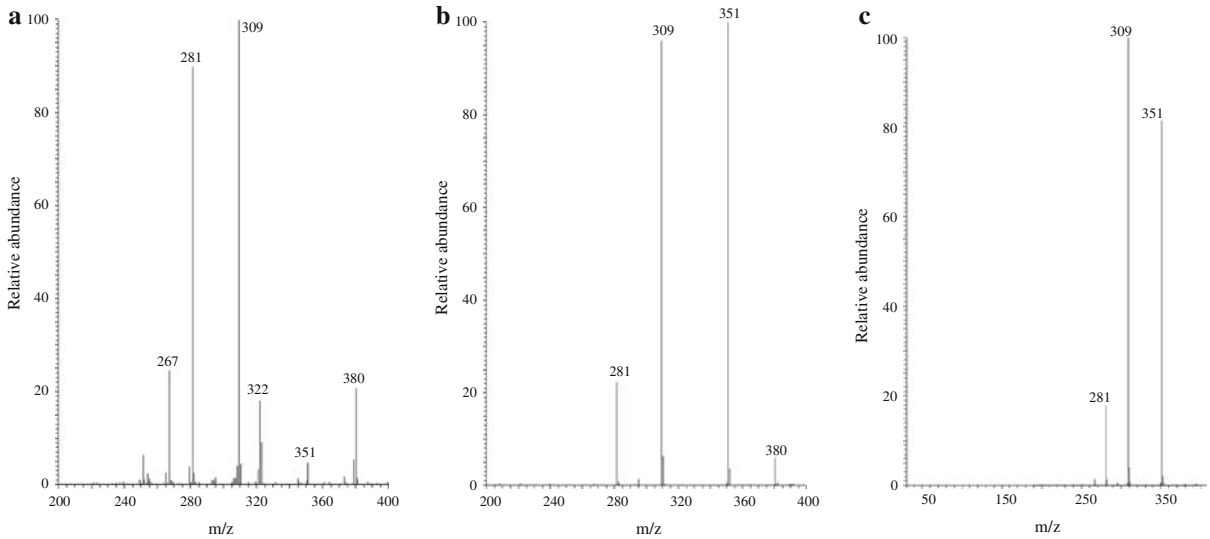

Fig. 4 Mass spectra obtained by GC-MS-MS analysis. (**a**) metabolites; (**b**), *p*353NC; (**c**), *p*353NR

HPLC-MS chromatograms of both *p*353NC and *p*353NR showed a peak at 14.9 min, which co-eluted with the isolated metabolites. The MS spectra at CID 20 eV showed the pseudomolecule peak $[M\text{-}H]^-$ at *m/z* 235 for the metabolite. The UV spectra of both reference compounds were similar. As shown in Fig. 3, the *p*353NC UV spectrum resembled that of the *p*353NP metabolites with a maximum absorption at ca. 280 nm.

GC-FTIR comparison of the metabolites with the reference compounds

Further comparison of the metabolites with the parent compound *p*353NP and the *p*353NC and *p*353NR reference compounds was achieved by means of GC-FTIR (Fig. 5). Parent compound *p*353NP emerged after 23.7 min well separated from the other compounds. The metabolites gave one peak with a retention time of 25.8 min; the diastereomers were not separated under these conditions. The IR spectra of the metabolites and of the *p*353NC (R_t 25.5 min) differed only little. The reference compound *p*353NR eluted after 26.2 min and exhibited additional bands at 2,350, 2,375, and 3,650 cm^{-1}. These differences however, were difficult to interpret due to the derivatisation necessary for gas chromatographic analysis. On the whole, all compounds demonstrated the 1,500 and 1,600 cm^{-1} bands of C–C valence vibrations of aromatic rings and bands between 2,970 and 2,880 cm^{-1} for alkyl C–H bonds. Moreover, a band for asymmetrical aromatic ring trisubstitution was also present at 850 cm^{-1}, such band is absent for vicinal trisubstitution. Thus, *p*353NP metabolites with three adjacent substitution groups were excluded (Fig. 1d, e). Furthermore, the metabolites exhibited a distinct band around 1,230 cm^{-1} which argues against a symmetrical trisubstitution (Fig. 1f).

Further microbial transformation of the new metabolites

The last part of this work was to assess whether the observed metabolites are dead-end products or intermediates. Growth tests were performed by using either the isolated metabolites, *p*353NC or *p*353NR as substrates for cultures of *Sphingomonas* sp. strain TTNP3. Abiotic controls and cultures with *p*353NP (0.1 g/l) were performed simultaneously. At the start of experiments optical density at 550 nm was between 0.05 and 0.07. Within five days of incubation, the optical density increased only in assays grown on *p*353NP or on the isolated metabolites achieving optical densities at 550 nm of approximately 0.24 and 0.15, respectively. Extraction and subsequent GC-MS analyses revealed significant abiotic losses of metabolites (ca. 70%) showing that they are very

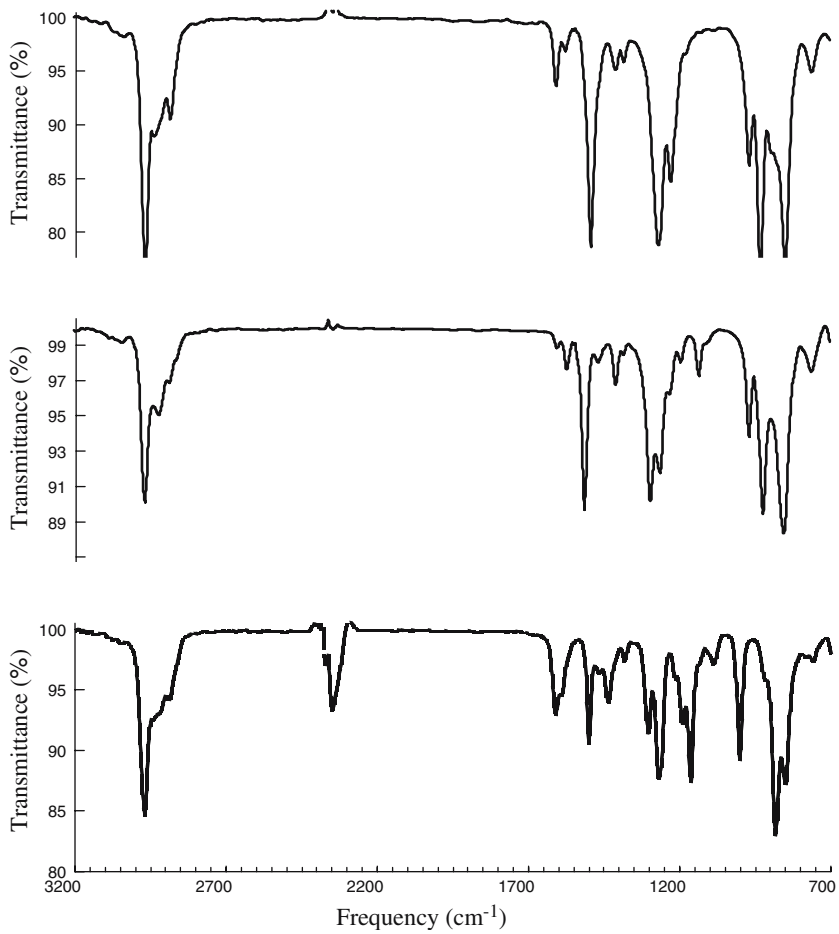

Fig. 5 Infrared spectra performed by GC-FTIR: metabolites (*top*), *p*353NC (*middle*) and *p*353NR (*bottom*)

unstable in aqueous solution. Since remaining portions could only be detected in abiotic assays, a minimum of 30% of the applied metabolites was degraded by *Sphingomonas* sp. strain TTNP3. These experiments thus clearly showed that the metabolites formed by *Sphingomonas* sp. strain TTNP3 are, from a biological point of view, different from *p*353NC and *p*353NR.

Conclusion

NP metabolism appears to vary, in dependence on the branching of the nonyl chain. An aromatic ring hydroxylation of octylphenol was reported in rainbow trout (Fereira-Leach and Hill 2001). The detoxification pathway lead to formation of alkylphenol glucuronide conjugates of octylcatechol. Such compounds were also detected in pond snail incubated with a single branched isomer of NP (Lalah et al. 2003). Side-chain hydroxylation products were reported in wheat cell suspension cultures on linear NP (Bokern et al. 1996). In bacterial consortia the formation of hydroxylated side-chain products of NPnEO have been reported, but the authors conceded that these metabolites resulted rather from less extensively branched nonyl chains (Di Corcia et al. 1998). Though till now, many assumptions have been formulated concerning ring attack during microbial metabolism of NP.

Concerning NP degradation by bacteria, most studies found in the literature report the extraction of NP metabolites from whole cellular suspensions or wastewater effluents containing microbial consortia (Di Corcia et al. 1998; Fujii et al. 2001; Tanghe et al. 2000; Corvini et al. 2004a). Such an approach allows mainly the extraction of compounds from the extracellular compartment. Some authors assumed that the metabolism of

amphiphilic compounds like NP leads to the excretion of lipophilic intermediates (Tanghe et al. 2000). Consequently, they expected their detection in the surrounding cell medium. However, substrates entering the cells do not always give rise to excretion of intermediary products, if they are comparatively rapidly metabolised. Another reason for the unsuccessful attempts to isolate further metabolites of NP was that these studies were performed with relatively small volumes of culture suspensions where metabolites, if present, were possibly present only in small amounts.

In the present study, we described the elements which contributed to establish the basis for the identification of the recently reported 2(3′,5′-dimethyl-3′-heptyl)-benzenediol (Corvini et al. 2004c). The use of high biomass cell suspension of *Sphingomonas* TTNP3 grown with tNP has been proven useful as it was the case for cells fed with *p*353NP for the preparation of intracellular extracts and the detection of ring hydroxylated metabolites. In the case of the cells fed with tNP, these metabolites could be detected by means of GC-MS as a group of peaks similar to the typical pattern observed for the tNP mixture. This fact was consistent with previous works reporting on the degradability of all isomers of tNP (Tanghe et al. 1999, Corvini et al. 2004a). LC-MS analyses of both intracellular extracts (cells grown in presence of tNP or *p*353NP) showed that these metabolites were oxidised products of NP. In addition, the UV spectra were characteristic for an intact aromatic moiety. GC-MS analyses of the derivatised extracts and corresponding mass calculations indicated that the products were doubly trimethylsilylated and thus consisted of hydroxylation products of tNP isomers or *p*353NP, accordingly. Due to the difficult gas chromatographic analyses and low peak resolution of the different metabolites a defined single isomer, i.e. *p*353NP was necessary for the further identification.

As previously described diastereomeric peaks were observed for the metabolites in the case of cells grown on *p*353NP (Corvini et al. 2004c). A more detailed examination of the mass spectra of the diastereomeric metabolites of *p*353NP showed that their fragmentation resembled that of *p*353NP. Thus, we assumed that the metabolites were ring hydroxylation products of diastereomeric *p*353NP. For the next step the chemical syntheses of the most probable metabolites of *p*353NP i.e. *p*353NC and *p*353NR were carried out. The metabolites obtained with *Sphingomonas* sp. strain TTNP3 cultivated on *p*353NP and the chemically synthesised putative metabolites *p*353NC and *p*353NR were compared by GC-FTIR and GC-MS-MS-analyses. The infrared spectra of the *p*353NC and the metabolites showed remarkable similarities and pointed to metabolites with 1,2,4-trisubstitution at the ring. GC-MS-MS analyses confirmed that no hydroxylation occurred at the alkyl chain and that most fragments emerged with *p*353NC, *p*353NR and isolated metabolites. However, slight differences in the relative abundance of these fragments led us to assume that the metabolites were different from *p*353NR and *p*353NC. First, ion at *m/z* 351 which results from the loss of ethyl at carbon 3′ of the nonyl chain was quite absent in the spectra of the metabolites. Furthermore, fragment at *m/z* 281 which corresponds to ethyl and pentyl losses for *p*353NP increased strongly in its relative abundance in the case of the metabolites. The corresponding fragment has also been found in the mass spectrum of nonylcatechol glucuronide conjugate after *β*-glucuronidase hydrolysis (Lalah et al. 2003). However, there the main ion resulted from a pentyl loss as in the case of the reference compounds *p*353NC and *p*353NR.

In contrast to *p*353NC and *p*353NR, biodegradation assays of the metabolites indicate that they were not dead end-metabolites and stimulated growth of *Sphingomonas* sp. strain TTNP3. However, it was not clear whether the metabolites were itself responsible for bacterial growth or if their abiotic transformation products served as the real substrates.

Based on these observations, two hypotheses are formulated. A structural rearrangement at the quaternary carbon atom (carbon 3′ of the nonyl chain) leads to a nonylcatechol with a rearranged alkyl chain (Fig. 1g). The hypothesis of structural rearrangement at this carbon occurring concomitantly or prior to hydroxylation could explain the formation of the corresponding nonanol, which is otherwise quite difficult to understand (Corvini et al. 2004a). Furthermore, transformation of the quaternary carbon into a less substituted carbon

atom adjacent to the ring could explain why this metabolite is further transformed by *Sphingomonas* sp. strain TTNP3 and *p*353NC was not. An intramolecular rearrangement of the propyl chain, which resembles the present possible rearrangement of *p*353NP metabolites, was described for bisphenol A (Lobos et al. 1992; Spivack et al. 1994). Another possible explanation for the formation of the observed metabolites could involve hydroxylation-induced migration referred to as NIH shift. NIH shifts were reported for halogenated as well as for alkyl substituents in the case of 4-methylphenylalanine as a consequence of aromatic ring hydroxylation catalysed by cytochrome P_{450} (Guroff et al. 1967, Koerts et al. 1998). Interestingly such enzymes are also present in the genus *Sphingomonas* (Imai et al. 2000). In the present case, such mechanism should lead to a 1,4 dihydroxylation product (Fig. 1h) where the alkyl chain could shift from C4 to an adjacent carbon atom. The last hypothesis could explain the formation of the 2(3′,5′-dimethyl-3′-heptyl)-benzenediol described recently (Corvini et al. 2004c).

Acknowledgements The authors wish to thank Dr J. Runsink and Mrs A. Müller for measurement of the NMR spectra at the Institute for Organic Chemistry and Maike Meindorf for her technical support. The work of LabMET was made possible by a grant from the FWO (Flemish Fund Scientific Research) n° **G.0102.00N.**

References

Bokern M, Nimtz M, Harms HH (1996) Metabolites of 4-n-nonylphenol in wheat cell suspension cultures. J Agric Food Chem 44:1123–1127

Corti A, Frassinetti S, Vallini G, D'Antone S, Fichi C, Solaro R (1995) Biotransformation of nonionic surfactants. I. Biotransformation of 4-(1-nonyl)phenol by *Candida maltosa* isolate. Environ Pollut 90:83–87

Corvini PFX, Vinken R, Hommes G, Schmidt B, Dohmann M (2004a) Degradation of the radioactive and non-labelled branched 3′,5′-dimethyl 3′-heptyl-phenol nonylphenol isomer by *Sphingomonas* TTNP3. Biodegradation 15:9–18

Corvini PFX, Vinken R, Hommes G, Mundt M, Meesters R, Schröder HF, Hollender J, Schmidt B (2004b) Microbial degradation of a single branched isomer of nonylphenol by *Sphingomonas* TTNP3. Water Sci Technol 50:195–202

Corvini PFX, Meesters RJW, Schäffer A, Schröder HFr, Vinken R, Hollender J (2004c) Degradation of a nonylphenol single isomer by *Sphingomonas* sp. strain TTNP3 leads to a hydroxylation-induced migration product. Appl Environ Microbiol 70:6897–6900

Dachs J, Van Ry DA, Eisenreich SJ (1999) Occurrence of estrogenic nonylphenols in the urban and coastal atmosphere of the lower Hudson River estuary. Environ Sci Technol 33:2676–2679

Di Corcia A, Costantino A, Crescenzi C, Marinoni E, Samperi R (1998) Characterization of recalcitrant intermediates of the branched alkyl side chain of nonylphenol ethoxylate surfactants. Environ Sci Technol 32:2401–2409

Ekelund R, Granmo Å, Magnusson K, Berggren M (1993) Biodegradation of 4-nonylphenol in seawater and sediment. Environ Pollut 79:59–61

Espadaler I, Caixach J, Om J, Ventura F, Cortina M, Pauné F, Rivera J (1997) Identification of organic pollutants in Ter river and its system of reservoirs supplying water to Barcelona (Catalonia, Spain): a study by GC/MS and FAB/MS. Water Res 31:1996–2004

Fereira-Leach AMR, Hill EM (2001) Bioconcentration and distribution of 4-*tert*-octylphenol residues in tissues of the rainbow trout (*Oncorhynchus mykiss*). Mar Environ Res 51:75–89

Fujii K, Urano N, Ushio H, Satomi M, Iida H, Ushio-Sata N, Kimura S (2000) Profile of a nonylphenol-degrading microflora and its potential for bioremedial applications. J Biochem 128:909–916

Fujii K, Urano N, Ushio H, Satomi M, Kimura S (2001) *Sphingomonas cloacae* sp. nov., a nonylphenol-degrading bacterium isolated from wastewater of a sewage-treatment plant in Tokyo. Int J Syst Evol Microbiol 51:603–610

Giger W, Ahel M, Koch M, Laubscher HU, Schaffner C, Schneider J (1987) Behaviour of alkylphenolpolyethoxylate surfactants and of nitrilotriacetate in sewage treatment. Water Sci Technol 19:449–460

Guroff G, Daly JW, Jerina DM, Renson J, Witkop B, Udenfriend S (1967) Hydroxylation-induced migration: the NIH shift. Science 157:1524–1530

Hesselsøe M, Jensen D, Skals K, Olesen T, Moldrup P, Roslev P, Krog Mortensen G, Henriksen K (2001) Degradation of 4-nonylphenol in homogeneous and nonhomogeneous mixtures of soil and sewage sludge. Environ Sci Technol 35:3695–3700

Imai Y, Matsunaga I, Kusunose E, Ichihara K (2000) Unique heme environment at the putative distal region of hydrogen peroxide-dependant fatty acid α-hydroxylase from *Sphingomonas paucimobilis* (peroxygenase $P450_{SP\alpha}$). J Biochem 128:189–194

Koerts J, Soffers AEMF, Vervoort J, De Jager A, Rietjens IMCM (1998) Occurrence of the NIH shift upon the cytochrome P450-catalyzed in vivo and in vitro aromatic ring hydroxylation of fluorobenzenes. Chem Res Toxicol 11:503–512

Lalah JO, Schramm KW, Severin GF, Lenoir D, Henkelmann B, Behechti A, Guenther K, Kettrup A (2003) In vivo metabolism and organ distribution of a branched ^{14}C-nonylphenol isomer in pond snails, *Lymnea stagnalis* L. Aquat Toxicol 62:305–319

Liber K, Knuth ML, Stay FS (1999) An integrated evaluation of the persistence and effects of 4-nonylphenol in an experimental littoral ecosystem. Environ Toxicol Chem 18:357–362

Lobos JH, Leib TK, Su TM (1992) Biodegradation of bisphenol A and other bisphenols by a gram-negative bacterium. Appl Environ Microbiol 58:1823–1831

Soto AM, Justica H, Wray JW, Sonnenschein C (1991) Para-nonylphenol: an estrogenic xenobiotic released from polystyrene. Environ Health Perspect 92:167–173

Spivack J, Leib TK, Lobos JH (1994) Novel pathway for bacterial metabolism of bisphenol A. J Biol Chem 269:7323–7329

Sundaram KMS, Szeto S (1981) The dissipation of nonylphenol in stream and pond water under simulated field conditions. J Environ Sci Health B16:767–776

Tanghe T, Devriese G, Verstraete W (1998) Nonylphenol degradation in lab scale activated sludge units is temperature dependent. Water Res 32:2889–2896

Tanghe T, Dhooge W, Verstraete W (1999) Isolation of a bacterial strain able to degrade branched nonylphenol. Appl Environ Microbiol 65:746–751

Tanghe T, Dhooge W, Verstraete W (2000) Formation of the metabolic intermediate 2,4,4-trimethyl-3-pentanol during incubation of a *Sphingomonas* sp. strain with the xeno-estrogenic octylphenol. Biodegradation 11:11–19

Topp E, Starratt A (2000) Rapid mineralization of the endocrine-disrupting chemical 4-nonylphenol in soil. Environ Toxicol Chem 19:313–318

Ushiba Y, Takahara Y, Ohta H (2003) *Sphingobium amiense* sp. nov., a novel nonylphenol-degrading bacterium isolated from a river sediment. Int J Syst Evol Microbiol 53:2045–2048

Vallini G, Frassinetti S, Scorzetti G (1997) *Candida aquaetextoris* sp. nov., a new species of yeast occurring in sludge from a textile industry wastewater treatment plant in Tuscany, Italy. Int J Syst Bacteriol 47:336–340

Van Ginkel CG 1996. Complete degradation of xenobiotic surfactants by consortia of aerobic microorganisms. Biodegradation 7:151–164

Vinken R, Schmidt B, Schäffer A (2002) Synthesis of tertiary ^{14}C-labelled nonylphenol isomers. J Label Compd Radiopharm 45:1253–1263

Wheeler TF, Heim JR, LaTorre MR, B Janes (1997) Mass spectral characterization of *p*-nonylphenol isomers using high-resolution capillary GC-MS. J Chromatogr Sci 35:19–30